Soft Matter

PAPER

Adhesion between highly stretchable materials†

Jingda Tang,[ab] Jianyu Li,[b] Joost J. Vlassak*[b] and Zhigang Suo*[bc]

Cite this: *Soft Matter*, 2016, **12**, 1093

Received 11th September 2015,
Accepted 4th November 2015

DOI: 10.1039/c5sm02305j

www.rsc.org/softmatter

Recently developed high-speed ionic devices require adherent laminates of stretchable and dissimilar materials, such as gels and elastomers. Adhesion between stretchable and dissimilar materials also plays important roles in medicine, stretchable electronics, and soft robots. Here we develop a method to characterize adhesion between materials capable of large, elastic deformation. We apply the method to measure the debond energy of elastomer–hydrogel bilayers. The debond energy between an acrylic elastomer and a polyacrylamide hydrogel is found to be about 0.5 J m^{-2}, independent of the thickness and the crosslink density of the hydrogel. This low debond energy, however, allows the bilayer to be adherent and highly stretchable, provided that the hydrogel is thin and compliant. Furthermore, we demonstrate that nanoparticles applied at the interface can improve adhesion between the elastomer and the hydrogel.

1. Introduction

Adhesion is ubiquitous in nature, engineering and medicine. Barnacles, kelp and mussels adhere to the surfaces of hard materials.[1] Wind turbines are assembled by bonding components of fiber-reinforced composites.[2] Damaged tooth tissues are bonded by adhesives.[3] Here we focus on adhesion between soft materials. In soft robots, elastomeric components adhere airtightly to form pneumatic chambers.[4] In stretchable electronics, soft devices form intimate contact with soft tissues (*e.g.*, skin, heart, brain, and spinal cord) to collect biometric data, as well as deliver drugs and electrical stimulation.[5,6] In established medical practices, soft materials adhere to soft tissues for mucus protection, ophthalmic surgeries, and wound dressing.[7–11] Recently, a family of stretchable, transparent, ionic devices has been demonstrated using dielectric elastomers layered with common salt-containing hydrogels,[12] water-retaining hydrogels,[13] or nonvolatile ionogels.[14] Applications include artificial muscles, skin and axons.[15–17]

These applications call for methods to characterize adhesion between highly stretchable materials. Subjected to loads, adherent materials may deform greatly before debonding. The peel test has been applied to determine adhesion between pieces of hydrogels and between medical tapes and skin.[18,19] The suitability of the peel test is often questioned. When a tape is subjected to a peeling force, the material bends when the peeling front arrives, and straightens after the peeling front moves away. For a dissipating material, such bending and straightening cause hysteresis, so that the work done by the peeling force dissipates mostly by hysteresis rather than by debonding.[20,21] When the peel test is applied to highly stretchable materials, often the stretchable materials are layered with much less stretchable tapes.[18] This setup provides support to the soft materials, but limits their stretchability; the relevance of the testing results to the applications of highly stretchable materials is unclear. The lap shear test is another widely used method.[22–24] However, the analysis of the lap shear test assumes small strains,[25] whereas elastomers and hydrogels undergo nonlinear and large deformation before debonding. Fracture mechanics of highly deformable materials has been reviewed recently, which provides further background for this work.[26,27]

Here we develop an experimental method to determine the debond energy of highly stretchable materials. Our setup closely resembles the ionic devices mentioned above, and provides a direct method to characterize adhesion in such devices. We apply the method to study the adhesion between an acrylic elastomer (VHB 4910, 3M) and polyacrylamide (PAAm) hydrogels. We find the debond energy to be independent of the thickness and cross-link density of the hydrogels. The debond energy (0.5 J m^{-2}) is rather low, compared to the fracture energy of the polyacrylamide hydrogel (about 100 J m^{-2}),[28] and to the fracture energy of the acrylic elastomer (about 1000 J m^{-2}).[29] We show, however, that such a low debond energy does allow the bilayer to be adherent and highly stretchable, provided that the hydrogel is compliant compared to the elastomer. Furthermore, we show that the debond energy between the acrylic elastomer and the PAAm hydrogel can be increased by spreading silica nanoparticles at

[a] *State Key Lab for Turbulence and Complex Systems, College of Engineering, Peking University, Beijing, 100871, China*
[b] *School of Engineering and Applied Sciences, Harvard University, Cambridge, MA 02138, USA. E-mail: vlassak@seas.harvard.edu, suo@seas.harvard.edu*
[c] *Kavli Institute of Bionano Science and Technology, Harvard University, Cambridge, MA 02138, USA*

† Electronic supplementary information (ESI) available. See DOI: 10.1039/c5sm02305j

the interface. We also characterize the adhesion between the acrylic elastomer and several other commonly used hydrogels, with or without nanoparticles.

2. Method to determine the debond energy

We prepare a laminate of two highly stretchable materials, with a small region left unbonded (Fig. 1a). We call one material film, the other material substrate, and the laminate bilayer. We then pull the substrate off the bilayer, and record the critical force for the advancement of debonding (Fig. 1b). We convert the critical force to the debond energy according to a procedure described below. We apply the method to a hydrogel film layered with an elastomer substrate (Fig. 1c, ESI,† Movies 1 and 2).

We assume that both materials deform elastically, and characterize their elasticity as follows. We pull the bare substrate by a uniaxial force, and measure the length of the deformed substrate. Let P be the force per unit width (*i.e.*, the force in the current state divided by the width of the substrate in the undeformed state). Let λ be the stretch (*i.e.*, the length of the substrate in the current state divided by the length of the substrate in the undeformed state). We record the force–stretch curve of the substrate, $P = P_s(\lambda)$. The area under the force–stretch curve, $U_s(\lambda) = \int_1^{\lambda} P_s(\lambda)\mathrm{d}\lambda$, is the elastic energy stored in the substrate divided by the area of the substrate in the undeformed state (Fig. 1d). We also record the force–stretch

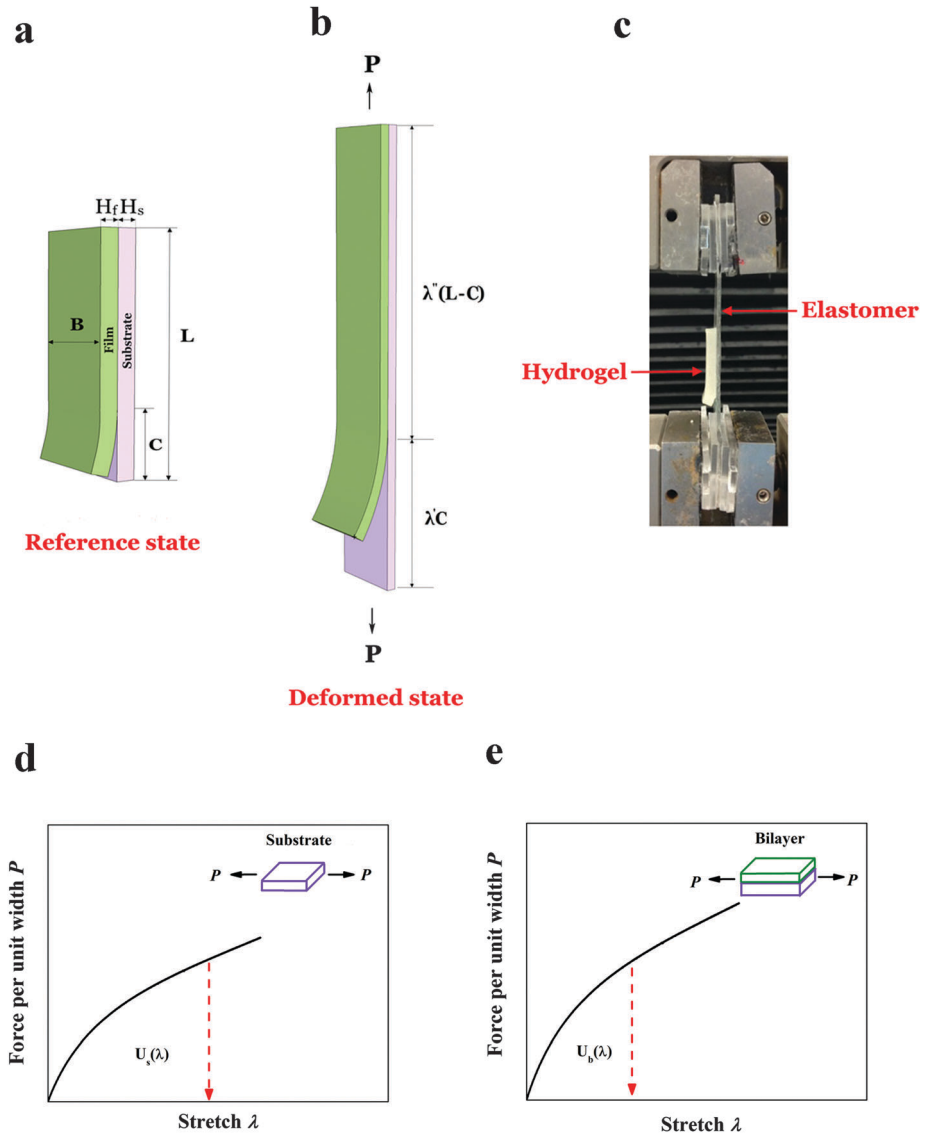

Fig. 1 Experimental method to determine the debond energy between two highly stretchable materials. (a) In the reference state, both materials are undeformed. (b) In a deformed state, the specimen is subjected to a force per unit width, P, the debonded substrate stretches by λ', and the bonded bilayer stretches by λ''. (c) An image of a bilayer consisting of a hydrogel film and an elastomer substrate. (d) Force–stretch curve of the substrate. The area under the curve is the elastic energy stored in the substrate. (e) Force–stretch relation of the bonded bilayer. The area under the curve is the elastic energy stored in the bilayer.

curve of the film, $P = P_f(\lambda)$. The area under the force–stretch curve, $U_f(\lambda) = \int_1^\lambda P_f(\lambda)d\lambda$, is the elastic energy stored in the film divided by the area of the film in the undeformed state. If the film is too fragile to handle, we can pull the film–substrate bilayer by a uniaxial force, and record the force–stretch curve of the bilayer, $P = P_b(\lambda)$. The area under the force–stretch curve, $U_b(\lambda) = \int_1^\lambda P_b(\lambda)d\lambda$, is the elastic energy stored in the bilayer divided by the area of the bilayer in the undeformed state (Fig. 1e).

The stretchable materials are taken as incompressible. Subjected to a uniaxial force, each material deforms in the longitudinal direction by stretch λ, and deforms in the two transverse directions by stretch $\lambda^{-1/2}$. This state of triaxial deformation exists in each material when it is pulled alone, and when two materials are pulled as a bilayer. Consequently, $P_s(\lambda) + P_f(\lambda) = P_b(\lambda)$ and $U_s(\lambda) + U_f(\lambda) = U_b(\lambda)$.

We next determine the energy release rate—that is, the reduction in the potential energy associated with debonding advancing by unit area. We choose to use the area in the undeformed state. In the undeformed state, the bilayer has a total length L, and the debonded region has a length C (Fig. 1a). In a current state, the bilayer is subjected to a constant force P, the detached substrate is stretched by λ', and the bonded bilayer is stretched by λ (Fig. 1b). The potential energy of the system consists of the elastic energy in the bilayer and the potential energy of the applied force. The potential energy of the detached substrate is $C[U_s(\lambda') - P\lambda']$, and that of the bonded bilayer is $(L - C)[U_b(\lambda'') - P\lambda'']$. Consequently, the energy release rate is

$$G = U_b(\lambda'') - U_s(\lambda') + P(\lambda' - \lambda''). \quad (1)$$

For writing the potential energy, we have assumed that the detached substrate is in a homogeneous state of stretch λ', and the attached laminate is in a homogeneous state of λ''. Around the debonding front, however, the field is inhomogeneous. Because the length of the debonded region is large compared to the thickness of the bilayer, the debond advances in a steady state—that is, the inhomogeneous field around the debonding front is invariant as debonding advances. Consequently, the inhomogeneous field around the debonding front does not affect the calculation of the energy release rate. As long as the sample is homogeneous along the length of the sample, the setup has translational symmetry. Consequently, the energy release rate is determined by an analytic expression (1); the user need not determine inhomogeneous deformation. Experimental setups with translational symmetry have been used extensively since the beginning of the fracture mechanics of rubberlike materials.[30]

In the limiting case that the substrate is much stiffer than the film, the attached film does not constrain the substrate, so that the stretch in the detached substrate is nearly the same as the stretch in the bonded bilayer, $\lambda' = \lambda'' = \lambda$. In this limiting case, the energy release rate reduces to $G = U_b(\lambda) - U_s(\lambda)$. If the difference in the energy stored in the bilayer and that in the substrate is too small to measure accurately, the direct measurement of the elastic energy stored in the film is desirable, and the energy release rate is $G = U_f(\lambda)$.

In the limiting case that the substrate is much softer than the film, the attached laminate does not deform, $\lambda'' = 1$, so that the energy release rate is entirely due to the detached substrate: $G = P(\lambda' - 1) - U_s(\lambda')$.

When the applied force reaches the critical value P_{cr} for the advancement of debonding, the energy release rate G reaches the debond energy Γ. Once the critical force P_{cr} is measured, we determine the associated stretch λ' from the force–stretch relation of the substrate (Fig. 1d), and the associated stretch λ'' from the force–stretch relation of the film–substrate bilayer (Fig. 1e). With known P_{cr}, λ' and λ'', we calculate the debond energy Γ using eqn (1).

This experimental method does not require mechanical testing of the film by itself; rather, the film can be tested together with the substrate as a bilayer. This fact is significant if we prepare the film directly on the substrate or if the film is too fragile to handle. Furthermore, the method allows both the film and the substrate to be inhomogeneous in the thickness direction, a feature that may be useful when testing very thin films that are inhomogeneous in the thickness direction. In this paper, we will choose elastic materials to demonstrate the method. Whether the method is suitable for highly dissipative materials remains to be studied.

3. Materials and the testing method

An acrylic elastomer (VHB 4910, 3M) thickness 1 mm, was purchased from McMaster-Carr. Acrylamide (AAm), *N*,*N*-dimethylacrylamide, *N*-isopropylacrylamide, acrylic acid, *N*,*N*′-methylenebis-(acrylamide) (MBAA), *N*,*N*,*N*′,*N*′-tetramethylethylenediamine (TEMED) and ammonium persulfate (APS) were acquired from Sigma Aldrich. Alginate was purchased from FMC BioPolymer company (USA). We prepared the polyacrylamide hydrogel samples using free radical polymerization. As a typical example, a polyacrylamide hydrogel with a MBAA/AAm weight ratio of 0.1% was synthesized by first preparing a 2.2 M aqueous solution of AAm. Then to this solution the MBAA crosslinker, TEMED, and APS were added (0.001, 0.0025, and 0.0042 times the weight of AAm, respectively). The solutions were then poured into a $75 \times 45 \times 3$ mm^3 plastic mold and covered with a glass plate. The samples were stored at room temperature for 24 hours to complete the polymerization process. Hydrogels with different crosslink densities and thicknesses were prepared by changing the amount of MBAA and the thickness of the mold. Similar procedures were used to prepare poly(*N*,*N*-dimethylacrylamide) (PDMA), poly(*N*-isopropylacrylamide) (PNIPAM) and polyacrylic acid (PAA) hydrogels. The PDMA-alginate hydrogel was prepared using the method described in ref. 28. We used a laser cutter to cut the hydrogels. The hydrogel samples had typical dimensions of $20 \times 10 \times 3.23$ mm^3.

The VHB tape was cut into ribbons with dimensions of $70 \times 10 \times 1$ mm^3. The gauge length of the specimens for the adhesion tests was 40 mm, as defined by the distance between the two polystyrene clamps. To create an unbonded region of length 3 mm at the interface, we placed a very thin plastic film ($3 \times 10 \times 0.1$ mm^3) between the hydrogel and the VHB ribbon. A hydrogel film was placed on top of a VHB ribbon and compressed firmly using a tweezer. All mechanical tests were

performed in air, at room temperature, using an Instron tensile tester with a 50-N load cell. The strain rate was kept constant 0.0125 s^{-1} for all the tensile tests. The adhesion tests were filmed using a digital camera and the videos were analyzed to determine the instance at which the unbounded region expands.

4. Debond energy is independent of the thickness and crosslink density of the hydrogel

We performed a series of uniaxial tensile tests on both the VHB elastomer and the PAAm hydrogels. The crosslink density of the PAAm hydrogels was varied by controlling the amount of the MBAA crosslinker; the ratio of the mass of the crosslinker to that of the monomer is denoted by N. Both the elastomer and the hydrogels are highly stretchable (Fig. 2a and b). As expected, the slope of the initial portion of the force–stretch curves of the hydrogel increases with the amount of MBAA (Fig. 2b).

We prepared bilayers with hydrogel layers of different thicknesses, H_f, and performed adhesion tests. The critical stretch for debonding the bilayer decreases significantly as the thickness of the hydrogel increases from $H_f = 0.1$ mm to $H_f = 0.6$ mm, and approaches a constant value for thicker hydrogels (Fig. 3c). In contrast to the critical stretch, the debond energy is independent of the thickness of the hydrogel film, and has a value

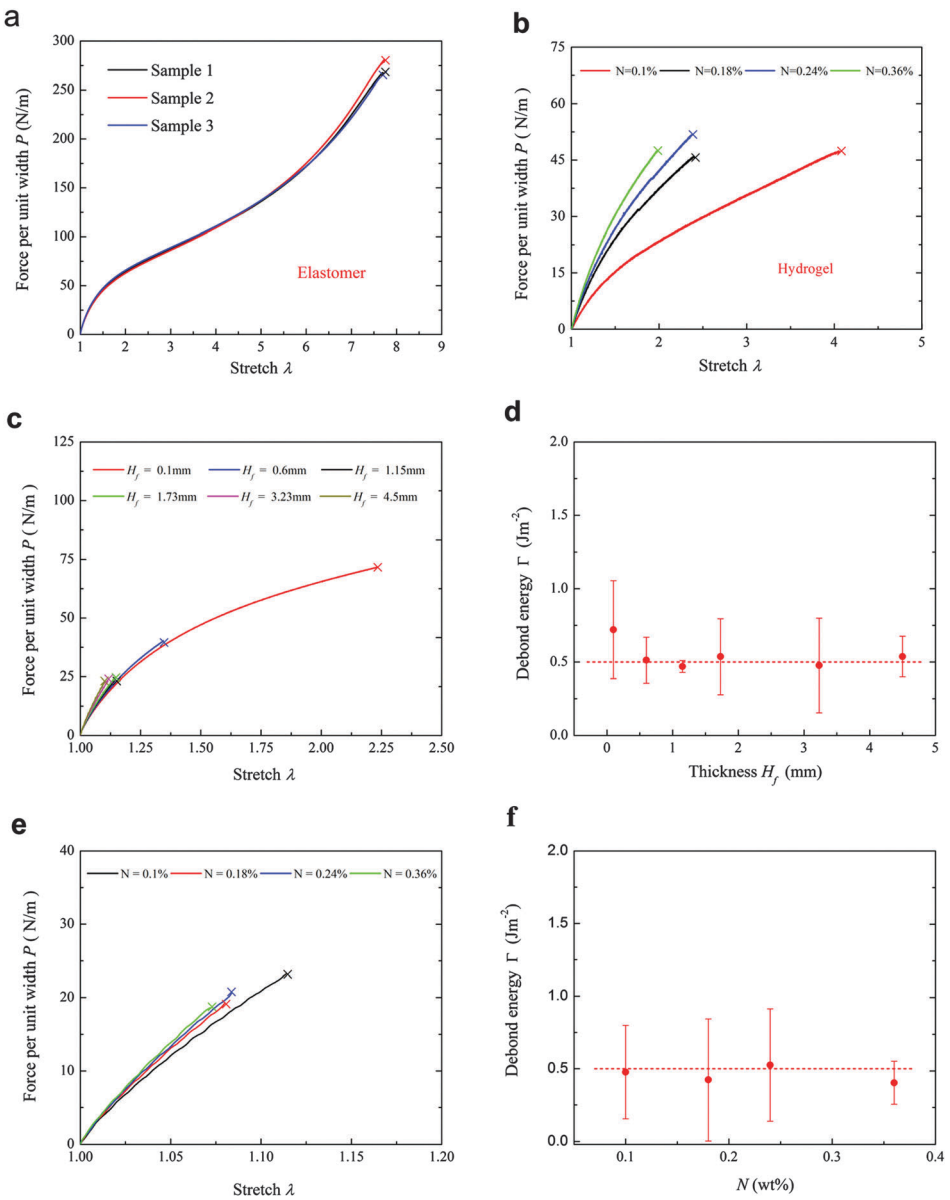

Fig. 2 Effect of the thickness and cross-link density of the hydrogels on the debond energy of the bilayer. (a) The force–stretch curve of the VHB. (b) The force–stretch curves of hydrogels with different MBAA/AAm weight ratios N. The thickness of the gels was 3.23 mm. (c) The force–stretch curves for the bilayers of VHB and hydrogels of several thicknesses. (d) The debond energy is independent of the thickness of hydrogel. (e) The force–stretch curve for the bilayer of VHB and hydrogels with different crosslink densities N. (f) The debond energy is independent of the crosslink density of the hydrogel.

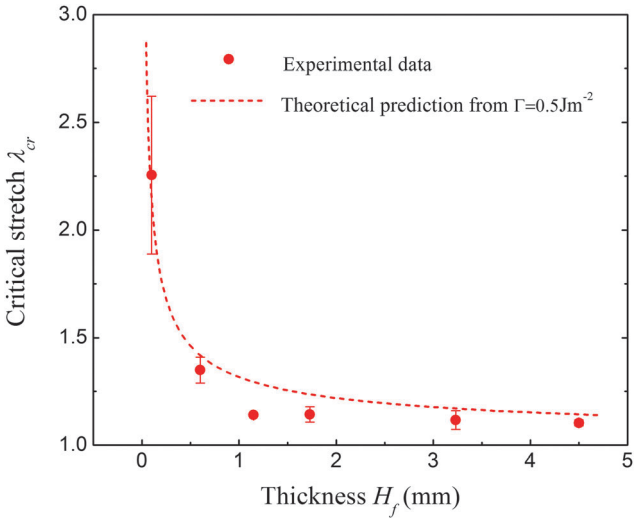

Fig. 3 The experimental data and the theoretical prediction of the critical stretch using constant debond energy for the PAAm hydrogel film with different thicknesses.

of approximately 0.5 J m^{-2} (Fig. 2d). This thickness independence supports the notion that the debond energy is a material constant. The debond energy, 0.5 J m^{-2}, is low compared to the fracture energy of polyacrylamide hydrogels (about 100 J m^{-2}),[28] and to the fracture energy of the acrylic elastomer (about 1000 J m^{-2}).[29] The low debond energy is not surprising, however, because the hydrogel and the elastomer interact through van der Waals forces.

Although the debond energy is low, the bilayer remains adherent and is highly stretchable, provided the hydrogel is thin (Fig. 2c, ESI,† Movie 3). The debond energy has units of energy per unit area, whereas the elastic energy density has units of energy per unit volume. Thus a thinner hydrogel stores less elastic energy, allowing the bilayer to stretch more before the hydrogel detaches. This result has important practical implications in that laminates with thinner films may sustain larger stretches for the same debond energy. This principle can guide the design of stretchable, layered structures. Epidermal electronics and transparent loudspeakers, for instance, have attached films of thicknesses of only 30 μm and 100 μm, respectively.[5,12]

We have evaluated the effect of hydrogel crosslink density on the debond energy. The MBAA/AAm weight ratio was changed from 0.1% to 0.36% for 3.23 mm-thick PAAm hydrogel films. Fig. 2e shows the force–stretch relation for the bilayer of VHB 4910 and the PAAm hydrogel with different crosslink densities. The debond energy is independent of the crosslink density of the PAAm hydrogel (Fig. 2f). This independence supports the notion that no polymer chains of the hydrogel penetrate into the elastomer, that the resistance to interfacial crack propagation is due to weak physical interaction, and that debonding propagates without breaking any polymer chains.

Once the debond energy Γ is measured, we can predict the critical stretch at which the hydrogel delaminates. Substituting the debond energy for the energy release rate in eqn (1), we obtain that $\Gamma = U_b(\lambda'') - U_s(\lambda') + P(\lambda' - \lambda'')$. The measured force–stretch relations for the bilayer and the bare substrate provide two additional equations, $P_{cr} = P_b(\lambda'')$ and $P_{cr} = P_s(\lambda')$. These three equations together determine the three unknown values: P_{cr}, λ' and λ''. In our experiments, the hydrogel film is very compliant relative to the elastomer substrate, so that λ' and λ'' are close. Write $\lambda' = \lambda'' = \lambda_{cr}$, the critical stretch is determined by $\Gamma = U_f(\lambda_{cr})$, where the function $U_f(\lambda) = \int_1^\lambda P_f(\lambda)d\lambda$ is calculated from the experimental force–stretch curve of the hydrogel, $P_f(\lambda)$. The calculated critical stretches agree well with the experimental data (Fig. 3).

5. Improving adhesion between the hydrogel and the elastomer using nanoparticles

Strategies to improve the adhesion between highly stretchable materials are under active investigation. Existing strategies include stimulation using the electric field, the double-network design of the interface, and the addition of an electrolytic polymer liquid.[19,31,32] J. Bacharouche *et al.* demonstrated that free radicals generated by plasma treatment of one PDMS substrate can provide good interfacial bonding to another PDMS layer such that delamination is effectively restrained under elongation/retraction cycles.[33] Recently, nanoparticle solutions have been used as adhesives for gels.[34] This approach is analogous to the strategy of improving the bulk properties of hydrogels using nanoclays or nanaoparticles.[35,36] These methods rely on the interaction between nanoparticles and polymer chains, which may involve hydrogen bonding and ionic adsorption.[35,37]

Here we demonstrate that silica nanoparticles can also improve adhesion between hydrogels and elastomers. The nanoparticles at a hydrogel/elastomer interface adsorb on the polymer chains of the hydrogel and the elastomer, forming physical bonds that bridge the interface (Fig. 4a). Those polymer chains need to detach from the nanoparticles for the hydrogel and the elastomer to debond. The nanoparticles can significantly improve adhesion if the nanoparticles attach well to the polymer chains of both the hydrogel and the elastomer.

We chose Ludox TM-50 (supplied by Sigma Aldrich) as the silica colloidal nanoparticle solution. The parameters of Ludox TM-50 have been well documented: silica concentrations of 50 wt% at pH 9, SiO_2/Na_2O ratios of 200–250, a radius of about 15 nm, a density of 1.4 g ml^{-1} and a surface area of 110–150 m^2 g^{-1}.[34,38] The surface of amorphous silica is quite complex and consists of different functional groups, including silanol groups (Si–OH).[39] The hydroxyl ions in the solution can react with the surface silanol groups to create negative charges to make the particles repel each other and disperse.[40] The zeta potential of Ludox TM-50 was measured to be about −35 mV at pH 9, confirming that the silica surface is highly negatively charged.[38]

We spread 20 μL of silica (Ludox TM-50) colloidal nanoparticle solution on the surface of the VHB, and attach the PAAm hydrogel on top. The MBAA/AAm weight ratio was changed from 0.1% to

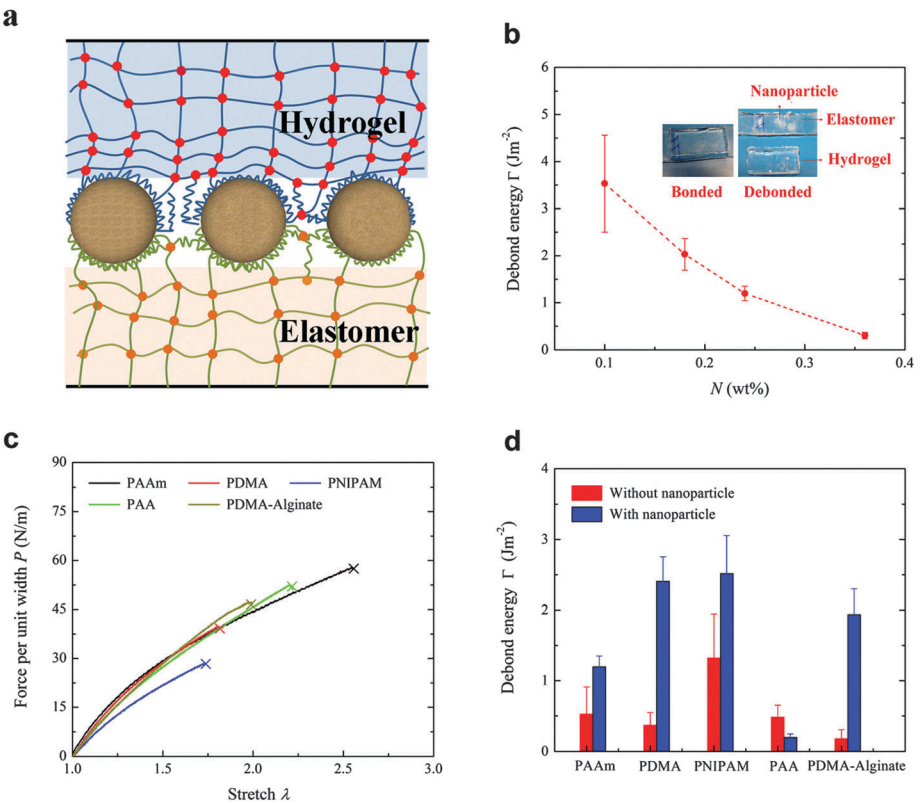

Fig. 4 Nanoparticles improve the adhesion between elastomer and hydrogel. (a) Polymer chains from both the elastomer and the hydrogel adsorb on the surface of the nanoparticles. (b) The debond energy of VHB–nanoparticle–PAAm interface as a function of MBAA/AAm weight ratios. The photo in the insets depicts the bonded and debonded specimens with nanoparticles. (c) The force–stretch curves of several types of hydrogels. (d) The effect of nanoparticles on the debond energy between VHB and different hydrogels, including the poly(*N*,*N*-dimethylacrylamide) hydrogel (PDMA), the poly(*N*-isopropylacrylamide) hydrogel (PNIPAM), the polyacrylic acid hydrogel (PAA) and the PDMA-alginate hybrid hydrogel.

0.36% for 3.23 mm thick PAAm hydrogel films. The inset of Fig. 4(b) depicts the bonded state and the detached state of specimens with nanoparticles at the interface. There are some nanoparticles left on both the surface of the VHB and the PAAm hydrogel after detachment. In contrast to the interface without nanoparticles, the debond energy now changes with hydrogel crosslink density (Fig. 4b): for PAAm hydrogel with N = 0.1%, the debond energy changes from 0.5 J m^{-2} to 3.5 J m^{-2}, a nearly sevenfold increase. For the PAAm hydrogel with N = 0.36%, however, the debond energy remains almost the same. An increase in the debond energy leads to an increase in stretchability; compare ESI,† Movies 1 and 4.

The decrease in debond energy with increasing crosslink density for bilayers using nanoparticles (Fig. 4b) can be understood in terms of the Lake–Thomas model.[41] Nanoparticles act as connectors between the elastomer and the hydrogel, and extra energy is dissipated when polymer chains detach from the surfaces of nanoparticles. Indeed, detaching only one monomer releases the tension in the whole polymer chain between two crosslinks.[34] For the hydrogel with lower crosslink density, the polymer chain between two crosslinks is longer, and more energy is dissipated. Thus, for a bilayer with nanoparticles at the interface, more loosely crosslinked hydrogels have larger debond energies.

We also assessed the adhesion between VHB and several other types of hydrogels, including poly(*N*,*N*-dimethylacrylamide) (PDMA), poly(*N*-isopropylacrylamide) (PNIPAM), polyacrylic acid (PAA), and PDMA-alginate. Taking the above discussion into consideration, we kept the crosslink density the same for each kind of hydrogel. We prepared gels with similar initial slopes in the force–stretch curves (Fig. 4c), indicating that the crosslink densities of these gels were indeed similar. In the absence of nanoparticles, the debond energy for all these cases is on the order of 1 J m^{-2} (Fig. 4d), indicating that the adhesion between the acrylic elastomer and these hydrogels is intrinsically weak, probably because of the weak van der Waals interactions between the interfaces. The addition of nanoparticles increases the debond energy between the acrylic elastomer and all these hydrogels, except the PAA hydrogel (Fig. 4d). This phenomenon can be understood as follows. The surface of silica nanoparticles is negatively charged,[42] and the polymer backbone of the PAA hydrogel carries a high density of negative charges at high pH (for Ludox TM-50, pH = 9).[43,44] The electrostatic repulsion between the nanoparticles and the PAA hydrogel decreases the debond energy. In contrast to the PAA hydrogel, the polymer backbones of the PAAm, PDMA, and PNIPAM hydrogels are neutral and do not form strong electrostatic interaction with the surface charge of the silica nanoparticles.

6. Conclusions

In summary, we have developed an experimental method for measuring the debond energy between highly stretchable materials. The method is applicable for materials capable of large, elastic deformations, and does not require the user to solve any boundary-value problem. The experimental setup closely resembles that used in stretchable ionic devices, and provides data of immediate importance to these devices. The debond energy between an acrylic elastomer and a polyacrylamide hydrogel is independent of the thickness and crosslink density of the hydrogel. The value of the debond energy is low, but still allows the bilayer to be adherent and highly stretchable. We further show that the adhesion between the elastomer and the hydrogel can be improved by spreading nanoparticles at the interface.

Acknowledgements

This work at Harvard was supported by MRSEC (DMR 14-20570), and by NSF (CMMI-1404653). Tang is supported by China Scholarship Council as a visiting scholar for two years at Harvard University.

References

1 G. P. Maier, M. V. Rapp, J. H. Waite, J. N. Israelachvili and A. Butler, *Science*, 2015, **349**, 628–632.
2 C. Kong, J. Bang and Y. Sugiyama, *Energy*, 2005, **30**, 2101–2114.
3 J. D. De Munck, K. Van Landuyt, M. Peumans, A. Poitevin, P. Lambrechts, M. Braem and B. Van Meerbeek, *J. Dent. Res.*, 2005, **84**, 118–132.
4 F. Ilievski, A. D. Mazzeo, R. F. Shepherd, X. Chen and G. M. Whitesides, *Angew. Chem.*, 2011, **123**, 1930–1935.
5 D.-H. Kim, N. Lu, R. Ma, Y.-S. Kim, R.-H. Kim, S. Wang, J. Wu, S. M. Won, H. Tao and A. Islam, *Science*, 2011, **333**, 838–843.
6 I. R. Minev, P. Musienko, A. Hirsch, Q. Barraud, N. Wenger, E. M. Moraud, J. Gandar, M. Capogrosso, T. Milekovic and L. Asboth, *Science*, 2015, **347**, 159–163.
7 G. Sun, X. Zhang, Y.-I. Shen, R. Sebastian, L. E. Dickinson, K. Fox-Talbot, M. Reinblatt, C. Steenbergen, J. W. Harmon and S. Gerecht, *Proc. Natl. Acad. Sci. U. S. A.*, 2011, **108**, 20976–20981.
8 H. Park and J. R. Robinson, *J. Pharm. Res.*, 1987, **4**, 457–464.
9 A. M. Oelker, J. A. Berlin, M. Wathier and M. W. Grinstaff, *Biomacromolecules*, 2011, **12**, 1658–1665.
10 N. A. Peppas and J. J. Sahlin, *Biomaterials*, 1996, **17**, 1553–1561.
11 H. Park and J. R. Robinson, *J. Controlled Release*, 1985, **2**, 47–57.
12 C. Keplinger, J.-Y. Sun, C. C. Foo, P. Rothemund, G. M. Whitesides and Z. Suo, *Science*, 2013, **341**, 984–987.
13 Y. Bai, B. Chen, F. Xiang, J. Zhou, H. Wang and Z. Suo, *Appl. Phys. Lett.*, 2014, **105**, 151903.
14 B. Chen, J. J. Lu, C. H. Yang, J. H. Yang, J. Zhou, Y. M. Chen and Z. Suo, *ACS Appl. Mater. Interfaces*, 2014, **6**, 7840–7845.
15 P. Brochu and Q. Pei, *Macromol. Rapid Commun.*, 2010, **31**, 10–36.
16 J. Y. Sun, C. Keplinger, G. M. Whitesides and Z. Suo, *Adv. Mater.*, 2014, **26**, 7608–7614.
17 C. H. Yang, B. Chen, J. J. Lu, J. H. Yang, J. Zhou, Y. M. Chen and Z. Suo, *Extreme Mechanics Letters*, 2015, **3**, 59–65.
18 B. Laulicht, R. Langer and J. M. Karp, *Proc. Natl. Acad. Sci. U. S. A.*, 2012, **109**, 18803–18808.
19 J. PingáGong, *Polym. Chem.*, 2011, **2**, 575–580.
20 H. R. Brown, *IBM J. Res. Dev.*, 1994, **38**, 379–389.
21 A. Gent and G. Hamed, *Polym. Eng. Sci.*, 1977, **17**, 462–466.
22 D. G. Barrett, G. G. Bushnell and P. B. Messersmith, *Adv. Healthcare Mater.*, 2013, **2**, 745–755.
23 C. E. Brubaker and P. B. Messersmith, *Biomacromolecules*, 2011, **12**, 4326–4334.
24 J. Simson, J. Crist, I. Strehin, Q. Lu and J. H. Elisseeff, *J. Orthop. Res.*, 2013, **31**, 392–400.
25 K. Kendall, *J. Phys. D: Appl. Phys.*, 1975, **8**, 512.
26 T. Zhang, S. Lin, H. Yuk and X. Zhao, *Extreme Mechanics Letters*, 2015, **4**, 1–8.
27 R. Long and C.-Y. Hui, *Extreme Mechanics Letters*, 2015, **4**, 131–155.
28 J.-Y. Sun, X. Zhao, W. R. Illeperuma, O. Chaudhuri, K. H. Oh, D. J. Mooney, J. J. Vlassak and Z. Suo, *Nature*, 2012, **489**, 133–136.
29 M. Pharr, J.-Y. Sun and Z. Suo, *J. Appl. Phys.*, 2012, **111**, 104114.
30 R. Rivlin and A. G. Thomas, *J. Polym. Sci.*, 1953, **10**, 291–318.
31 T.-A. Asoh and A. Kikuchi, *Chem. Commun.*, 2010, **46**, 7793–7795.
32 H. Tamagawa and Y. Takahashi, *Mater. Chem. Phys.*, 2008, **107**, 164–170.
33 J. Bacharouche, P. Kunemann, P. Fioux, M.-F. Vallat, J. Lalevée, J. Hemmerlé and V. Roucoules, *Appl. Surf. Sci.*, 2013, **270**, 64–76.
34 S. Rose, A. Prevoteau, P. Elzière, D. Hourdet, A. Marcellan and L. Leibler, *Nature*, 2014, **505**, 382–385, DOI: 10.1038/nature12806.
35 K. Haraguchi and T. Takehisa, *Adv. Mater.*, 2002, **14**, 1120.
36 L. Carlsson, S. Rose, D. Hourdet and A. Marcellan, *Soft Matter*, 2010, **6**, 3619–3631.
37 K. Haraguchi, H.-J. Li, K. Matsuda, T. Takehisa and E. Elliott, *Macromolecules*, 2005, **38**, 3482–3490.
38 G. Orts-Gil, K. Natte, D. Drescher, H. Bresch, A. Mantion, J. Kneipp and W. Österle, *J. Nanopart. Res.*, 2011, **13**, 1593–1604.
39 L. Zhuravlev, *Colloids Surf., A*, 2000, **173**, 1–38.
40 R. Helmuth, D. Stark, S. Diamond and M. Moranville-Regourd, *Contract*, 1993, **100**, 202.
41 G. Lake and A. Thomas, *Proc. R. Soc. London, Ser. A*, 1967, **300**, 108–119.
42 A. A. Vertegel, R. W. Siegel and J. S. Dordick, *Langmuir*, 2004, **20**, 6800–6807.
43 J. Ricka and T. Tanaka, *Macromolecules*, 1984, **17**, 2916–2921.
44 J. Li, Z. Suo and J. J. Vlassak, *Soft Matter*, 2014, **10**, 2582–2590.